We are IntechOpen, the world's leading publisher of Open Access books Built by scientists, for scientists

6,900
Open access books available

185,000
International authors and editors

200M
Downloads

154
Countries delivered to

Our authors are among the

TOP 1%
most cited scientists

12.2%
Contributors from top 500 universities

CLARIVATE ANALYTICS
BOOK CITATION INDEX
INDEXED

WEB OF SCIENCE™

Selection of our books indexed in the Book Citation Index
in Web of Science™ Core Collection (BKCI)

Interested in publishing with us?
Contact book.department@intechopen.com

CFD Simulation of Flows in Stirred Tank Reactors Through Prediction of Momentum Source

Weidong Huang and Kun Li

Additional information is available at the end of the chapter

http://dx.doi.org/10.5772/51754

1. Introduction

The mixing and agitation of fluid in a stirred tank have raised continuous attention. Starting with Harvey and Greaves, Computational Fluid Dynamics (CFD) has been applied as a powerful tool for investigating the detailed information on the flow in the tank [1-2]. In their work, the impeller boundary condition (IBC) approach has been proposed for the impeller modeling, in which the flow characteristics near the impeller are experimentally measured, and are specified as the boundary conditions for the whole flow field computation [1-4]. Because it depends on the experimental data, IBC can hardly predict the flow in the stirred tank and its applicability is inherently limited. To overcome this drawback, the multiple rotating reference frames approach (MRF) has been developed, in which the vessel is divided into two parts: the inner zone using a rotating frame and the outer zone associated with a stationary frame, for a steady state simulation. Although it can predict the flow field, the computation result is slightly lack of accuracy and needs a longer time for convergence [5]. Sliding mesh approach (SM) is another available approach, in which the inner grid is assumed to rotate with the impeller speed, and the full transient simulations are carried out [6-7]. SM approach gives an improved result, but it suffers from the large computational expense [8]. Moving-deforming grid technique was proposed by Perng and Murthy [9], in which the grid throughout the vessel moves with the impeller and deforms. This approach requires a rigorous grid quality and the computational expenses are even higher than SM [10-11].

Momentum source term approach adds momentum source in the computational cells to represent the impeller propelling and the real blades are ignored. In the approach, the generations of the vessel configuration and grids are simpler, and the computational time is shorter and the computational accuracy is higher. However, the determination of the momentum source depends on experimental data or empirical coefficients presently [12-13]. The ap-

proach proposed by Pericleous and Patel is based on the airfoil aerodynamics and originally aimed at the two-dimensional flow in the stirred vessels. Xu, McGrath [14] and Patwardhan [15] applied this approach to simulate the three-dimensional flow pattern in a tank with the pitched blade turbines. Revstedt et al. [16] modified the approach for the three-dimensional simulation in a Rushton turbine stirred vessel. In their approach, the determination of the momentum source depends on the specified power number. Dhainaut et al. [13] reported a kind of momentum source term approach in which the fluid velocity is linearly proportional to the radius with an empirical coefficient. In our previous study, we proposed to calculate the momentum source term according to the ideal propeller equation [17], which is related to the rotation speed and radius of the blade [18-20], however, the prediction accuracy is just a little better than MRF method.

Besides, other methods, such as inner-outer approach, snapshot approach and adaptive force field technique, have been developed, but are less applied[1, 21].

In this study, an equation is proposed to calculate the momentum source term after considering both impeller propelling force and the radial friction effect between the blades and fluid. The flow field in the Rushton turbine stirred vessel was simulated with the CFD model. The available experimental data near the impeller tip and in the bulk region were applied to validate this approach. Moreover, the comparisons of the computational accuracy and time with MRF and SM were carried out.

2. Model and methods

2.1. Stirred tank and grid generation

Fig.1 shows the geometry of the investigated standard six-bladed Rushton turbine stirred tank with four equally spaced baffles. The diameter of cylindrical vessel $T = 0.30$ m, the diameter of rotating shaft $d = 0.012$ m, the hub diameter $b = 0.020$ mm, and the detailed size proportions are listed in Table 1. The working fluid is water with density $\rho = 998.2$ kg m^{-3} and viscosity $\mu = 1.003 \times 10^{-3}$ Pa s. The rotational speed of the impeller $N = 250$ rpm, leading to a tip speed $u_{tip} = 1.31$ m s^{-1} and Reynolds number Re = 41,467 (Re = $\rho N D^2 / \mu$). Eight axial locations in the bulk region are also shown in Fig.1. They are the same as the experimental study of Murthy and Joshi [22],

It is well known that sufficiently fine grids and lower-dissipation discretization schemes can significantly reduce the numerical errors [23]. And the grid resolution on the blades has an important influence on capturing the details of flow near the impeller [23-24]. Grid independence study has been carried out for momentum source term approach with the standard k-ε model with different grid resolutions. In this paper, the results of the grid resolution of 1,429,798 hexahedral cells ($r \times \theta \times z \approx 88 \times 120 \times 131$) with the impeller blade covered with 96000 cells ($r \times \theta \times z = 32 \times 120 \times 25$) have been reported for the simulations of standard k-ε model and Reynolds stress model (RSM). In the region encompassing the impeller discharge stream, contained within 1.5 blade heights above and below the impeller and extending hor-

izontally across the tank, the grid was refined to resolve the large flow gradients (Fig.2). For it is unnecessary to construct the impeller in momentum source term approach, the tank geometry and mesh generations are simpler than MRF and SM.
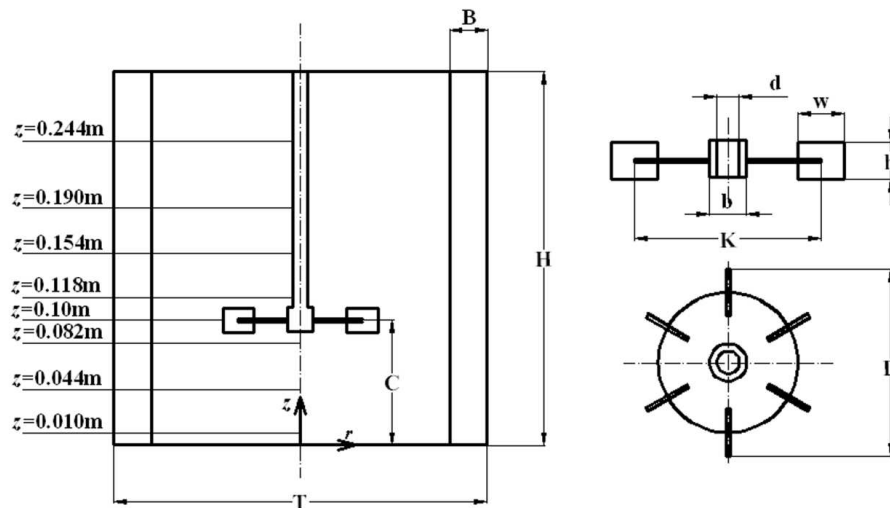

Figure 1. Geometry of the stirred vessel.

H/T	C/T	B/T	D/T	K/D	w/D	h/D
1	1/3	1/10	1/3	3/4	1/4	1/5

Table 1. Dimension scaling of the stirred vessel configuration.
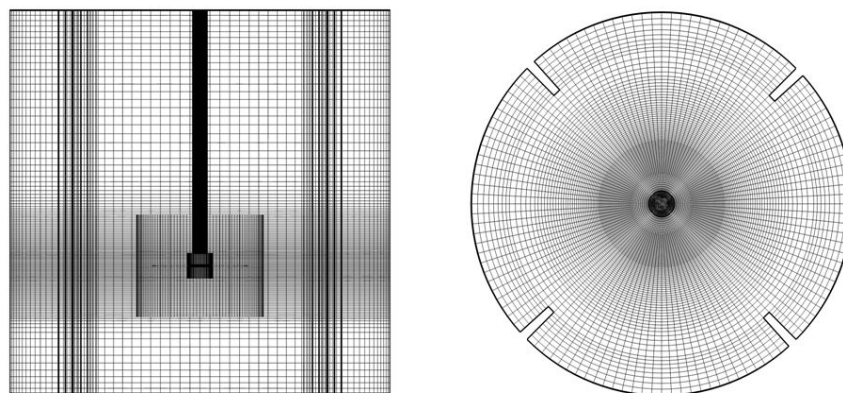

Figure 2. Computational mesh for the momentum source term approach simulation.

In order to investigate the computational speed of MRF and SM, they are also applied to simulate the flow field of stirred tank. The total number of computational cells for MRF is 1,652,532 ($r \times \theta \times z \approx 63 \times 204 \times 126$) with the impeller blade covered with 88128 cells ($r \times \theta \times z =$

24×204×18), and for SM is 606,876 ($r \times \theta \times z \approx$ 60×106×90) with the impeller blade covered with 33920 cells ($r \times \theta \times z$ = 20×106×16).

2.2. Momentum source model and control equations

Following the assumptions of Euler equation for turbomachinery [25], the momentum source term from the driving of blade is determined as following. For a small area of blade dS, assuming that a force exerted by the impeller on the fluid is perpendicular to the blade surface [14], the propelling force from the impeller dF is considered to be equal to the product of the mass flow rate across the interaction section dQ and the fluid velocity variation along the normal direction of the area element dS:

$$\mathrm{d}F = \mathrm{d}Q \cdot \Delta \vec{u} \tag{1}$$

Since the rigid body rotational motion of the blade is considered, it is a reasonable assumption that the fluid velocity after being acted on is the same as the velocity of the impeller blade, thus Δu can be obtained. For the present study on the vertical blade, Eq.(1) can be written as:

$$\mathrm{d}F = \rho \cdot \mathrm{d}S \cdot u \cdot (u - v_\theta) \tag{2}$$

where u is linear velocity of the area element on the blade surface dS, v_θ is fluid tangential velocity rotating with the impeller before the fluid was propelled by impeller, dS is cross-section area of the interface between fluid and the impeller blade. A similar equation has been applied to describe the propelling effect of the ship's impeller [26] which we applied it to calculate the momentum source term [18-19].

Furthermore, the fluid is continuously impelled out from the impeller region, so there is a relative motion of the fluid along the radial direction of the blade. In order to consider the friction effect on the fluid movement, the friction resistance equation about the finite flat plate based on the boundary layer theory is introduced to calculate the friction force approximately [27]:

$$\mathrm{d}f = \frac{1}{2}\rho v_r^2 \cdot C_f \cdot \mathrm{d}S \tag{3}$$

where f is friction force in the computational cells; v_r is radial velocity of the fluid; C_f is local resistance coefficient related to Re_x, which is calculated approximately by:

$$C_f = 0.664 \cdot \mathrm{Re}_x^{-0.5}$$
$$\mathrm{Re}_x <= 5 \times 10^5 \tag{4}$$

$$C_f = 0.0577 \cdot \mathrm{Re}_x^{-0.2}$$
$$5 \times 10^5 < \mathrm{Re}_x < 1 \times 10^7$$

(5)

where $\mathrm{Re}_x = \rho v_r x / \mu$, x is distance between cell center and the center of rotation axis. In this paper, we mainly consider the radial friction resistance, ignoring the axial effect for simplicity. Adding the momentum sources of the both direction into the computational cells, the real blade is replaced.

In the previous study, the difference between the ensemble-averaged flow field calculated with the steady-state and the time-dependent approaches was found to be negligible [28-30]. Here, the continuity and momentum equations of motion for three-dimensional incompressible flow, as well as the standard k–ε turbulence equation [31] or Reynolds stress transport equations [32], were solved to calculate single phase flow of the stirred vessel.

The free surface was treated as a flat and rigid lid, so a slip wall was given to the surface. The disc, hub and shaft of the Rushton turbine are specified as moving walls. A standard wall function was given to the other solid walls, including the bottom surface, the sidewall and baffles. Second order upwind discretization scheme was adopted for pressure interpolation and the convection term of momentum, turbulent kinetic energy and energy dissipation rate equations, and the discretized equations were solved iteratively by using the SIMPLE algorithm for pressure-velocity coupling.

2.3. Power number prediction

The power number N_P is an important parameter of the stirred tank, which is generally applied to validate the CFD predictions [33-34]. One method for calculating the power number is based on the energy balance, in which the power number of the impeller is calculated from the integration of the turbulent energy dissipation rate (ε) predicted from the CFD model [35]:

$$N_P = \frac{\int_0^H \int_0^{2\pi} \int_0^{T/2} \rho \varepsilon r \, dr \, d\theta \, dz}{\rho N^3 D^5}$$

(6)

In MRF and SM approaches, the power number is usually calculated from the predicted torque [36]:

$$N_p = \frac{2\pi N m M}{\rho N^3 D^5}$$

(7)

in which m is the number of the blades, M is the torque of each blade.

In the present study, since the force from blade results in the fluid movement, the impeller power can be calculated from the integration of the momentum source in the impeller re-

gion [14], which is called integral power based approach, so the power number is calculated in the following manner in our study:

$$N_p = \frac{\int_{C-h/2}^{C+h/2} \int_0^{2\pi} \int_{D/2-w}^{D/2} (F_\theta \cdot 2\pi Nr) r\mathrm{d}r\mathrm{d}\theta\mathrm{d}z}{\rho N^3 D^5} \qquad (8)$$

in which F_θ is tangential momentum source term.

3. Results and discussion

3.1. Numerical validation of the flow field near the impeller tip

Fig.3 shows the profiles of the predicted and experimental flow data in the impeller region. Fig.3a gives the comparison of the radial velocity. Escudie and Line [37] summarized the previous experimental works and found due to the differences of the experimental technique and the stirred-vessel configuration, there existed some inconsistencies among the reported results, whereas the maximum of radial velocity was in the range of 0.7-0.87u_{tip}. Their experiment study gave a maximal radial velocity of 0.80u_{tip}, while Wu and Patterson [38] 0.75u_{tip}. In present work, momentum source term approach with standard k-ε and RSM predicts a maximum radial velocity of 0.79u_{tip} and 0.75u_{tip}, respectively, which means that momentum source term approach predicts the maximal radial velocity rather well. From fig. 3a, the distribution of radial velocity predictions based on momentum source term approach agrees rather well with the experimental data, which outperforms MRF predictions.

With regard to tangential velocity, the maxima from Wu and Patterson [38], and Escudie and Line [37] are 0.66u_{tip} and 0.72u_{tip} respectively. For momentum source term approach with standard k-ε and RSM, both gave a maximum of 0.63u_{tip}. From Fig. 3b, it can be found that the calculated results of momentum source term approach are in good agreement with the two sets of experimental data, better than MRF predictions.

Fig.3c shows the comparison of axial velocity. The measured results from Wu and Patterson [38], Escudie and Line [37] are almost the same. The momentum source term approach results match the measured data well in most regions, but predicting the change from the maximum to minimum with several deviations. Compared to standard k-ε model, RSM predictions of momentum source term approach make some improvements, while MRF predictions are not provided.

In fig.3d, it can be observed that there are two maxima of different magnitudes in the profiles of turbulent kinetic energy, thus the curve is not symmetrical. RSM simulations of momentum source term approach are in accordance with those of standard k-ε model. Momentum source term approach and MRF both successfully predict the variations between two maxima, but momentum source term approach exhibits a better prediction of the turbulent kinetic energy than MRF.
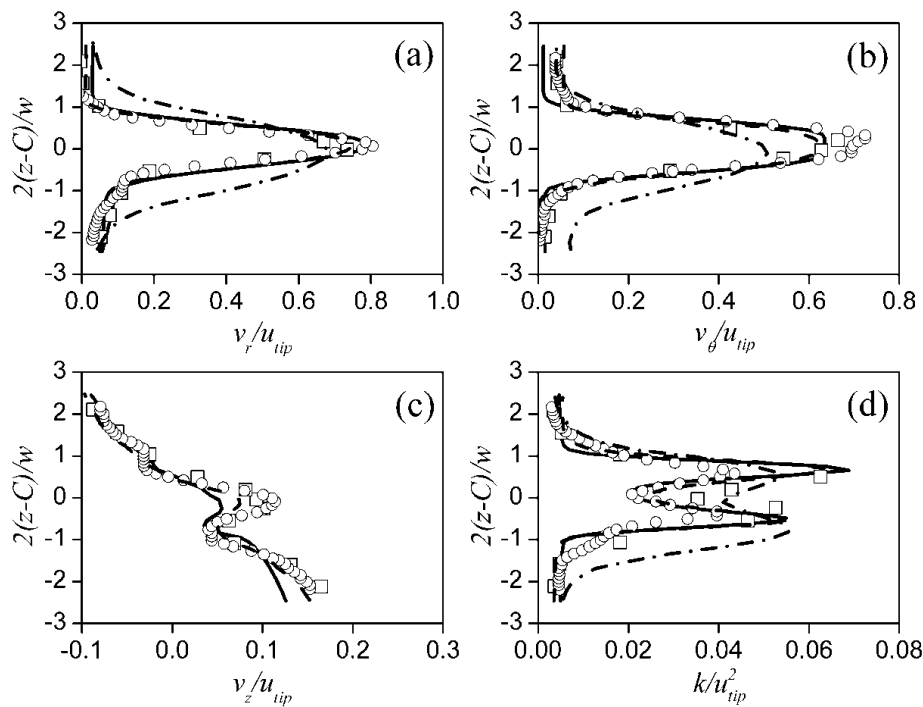
Figure 3. Comparison of the results predicted by different impeller approaches and experimental data around impeller tip (a) radial velocity, (b) tangential velocity, (c) axial velocity and (d) turbulence kinetic energy: ○ experimental data (Escudie and Line, 2003), ▪ experimental data (Wu and Patterson, 1989), standard k-ε momentum source term approach predictions, RSM momentum source term approach predictions, MRF predictions (Deglon and Meyer, 2006)

3.2. Numerical validation of the flow field in the bulk region

Fig.4 shows the radial profiles of the mean axial velocity at various axial levels. Here, $z<0.10$ m is in the lower parts of the tank, while $z>0.10$ m is in the upper parts. It can be noted that curve changes in two parts are just opposite, indicating that axial velocity directions are opposite. The result shows that the predictions of momentum source term approach with standard k-ε model and RSM are both in favorable agreement with the experimental data, similar to the predicted results of SM.

Fig.5 depicts the comparison of predicted and experimental radial velocity component. The high speed impeller discharge streams radially. Radial velocity initially increases and then decreases, attaining the maximum at $r/R = 0.6$-0.8 near blade. It can be seen that compared to the experimental data, both the standard k-ε model predictions of momentum source term approach and SM exhibit some disparity, particularly at the levels in the upper part. At the top axial levels ($z = 0.154$ m and $z = 0.244$ m), there are the largest differences between the predictions of momentum source term approach and SM, while they have similar accuracy in other positions. However, the results of momentum source term approach and SM predicted with RSM are consistent with the experimental data.
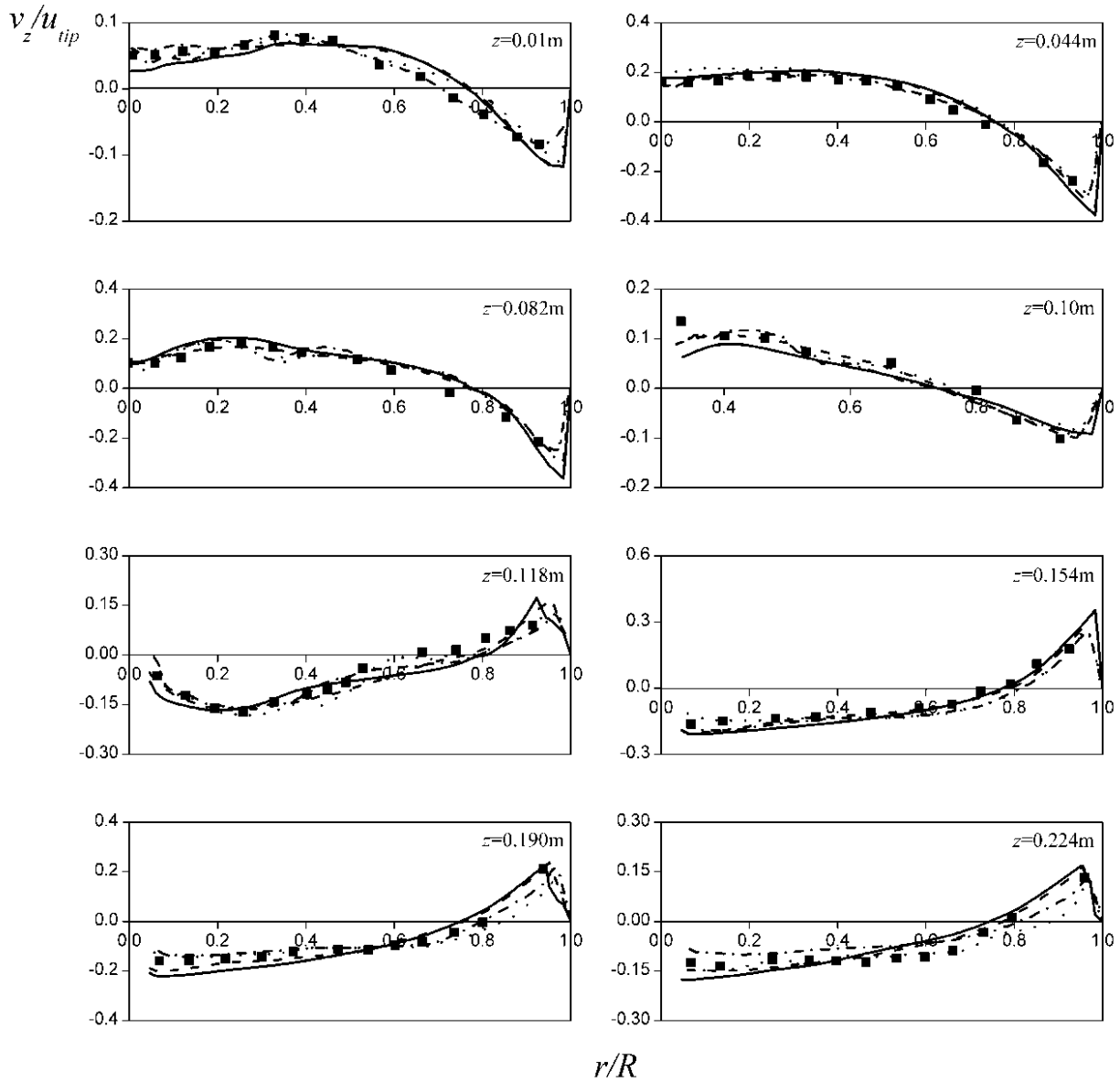
Figure 4. Comparison of the results predicted by different impeller approaches and experimental data of the dimensionless mean axial velocity in the bulk region: experimental data [39] (Murthy and Joshi, 2008) standard k-ε momentum source term approach predictions, RSM momentum source term approach predictions, standard k-ε SM predictions (Murthy and Joshi, 2008), RSM SM predictions (Murthy and Joshi, 2008).
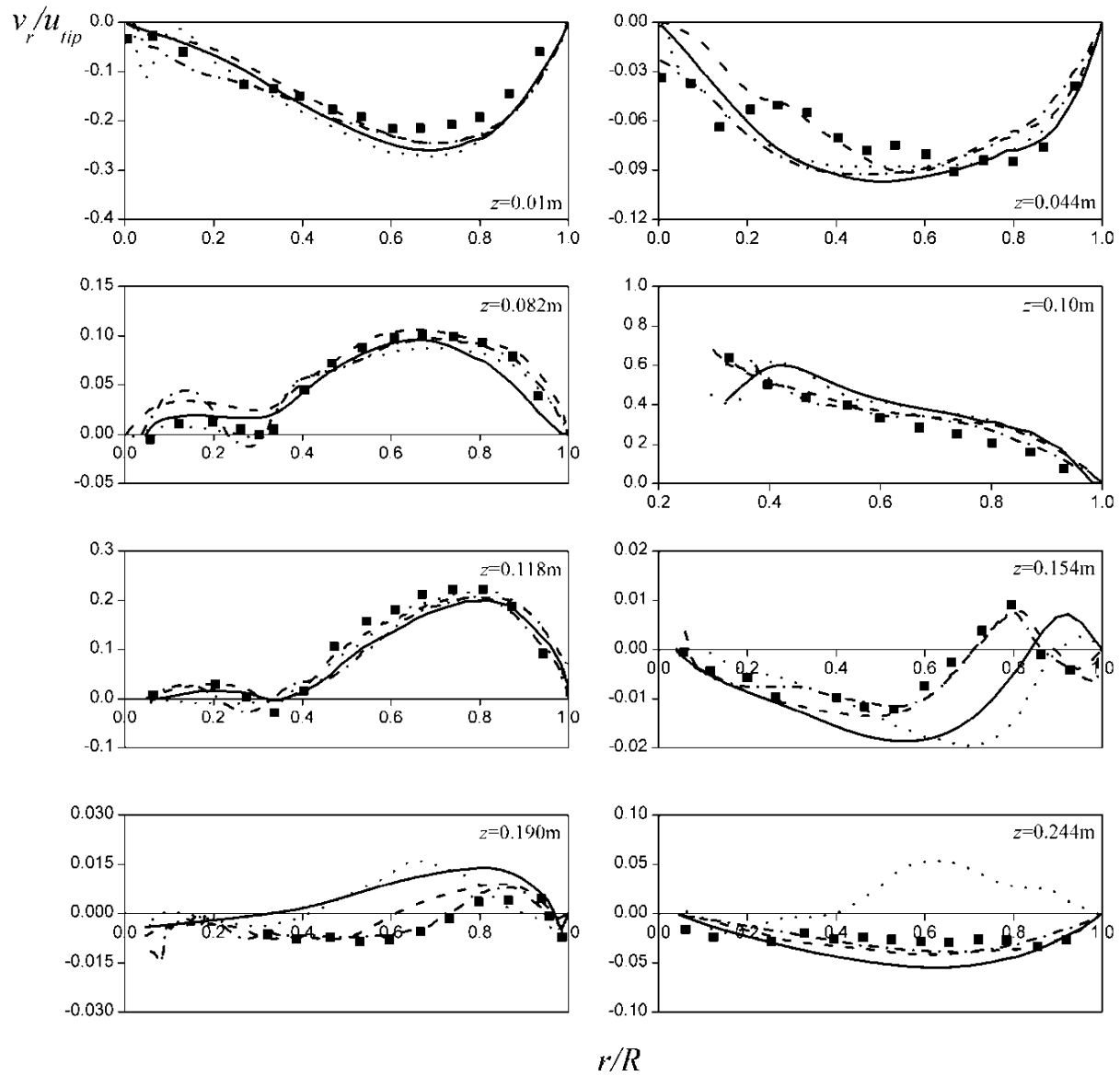
Figure 5. Comparison of the results predicted by different impeller approaches and experimental data of the dimensionless mean radial velocity in the bulk region: experimental data (Murthy and Joshi, 2008) standard k-ε momentum source term approach predictions, RSM momentum source term approach predictions, standard k-ε SM predictions (Murthy and Joshi, 2008), RSM SM predictions (Murthy and Joshi, 2008).
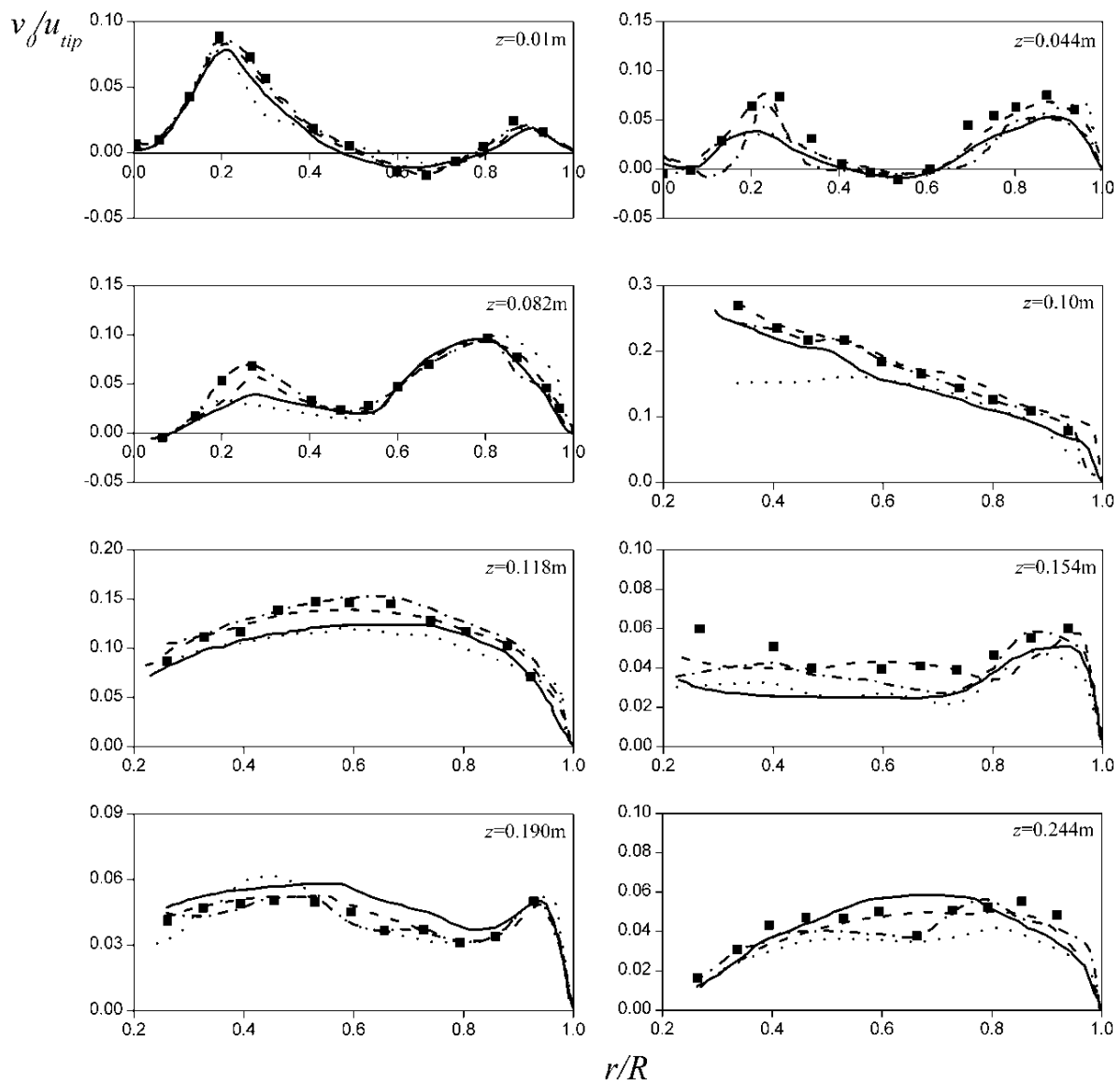
Figure 6. Comparison of the results predicted by different impeller approaches and experimental data of the dimensionless mean tangential velocity in the bulk region: experimental data (Murthy and Joshi, 2008) standard *k-ε* momentum source term approach predictions, RSM momentum source term approach predictions, standard *k-ε* SM predictions (Murthy and Joshi, 2008), RSM SM predictions (Murthy and Joshi, 2008).

Fig.6 illustrates the radial profiles of the tangential velocity component. Yianneskis et al [40] pointed out that the baffles reduce the vessel cross-section, which results in higher values for tangential velocity and a reduced pressure, thus generating reverse flows. It may be the reason that negative velocities exist at the levels of $z = 0.01$ m and $z = 0.044$ m. It can be seen that the computational results of momentum source term approach and SM with standard k-ε model are similar, and both of them predict the reverse flows. They agree rather well with the experimental data at the lower levels, whereas deviate at the upper levels. For RSM simulations, the prediction accuracy of two modeling methods have been improved, and their results are in good agreement with the experimental results.
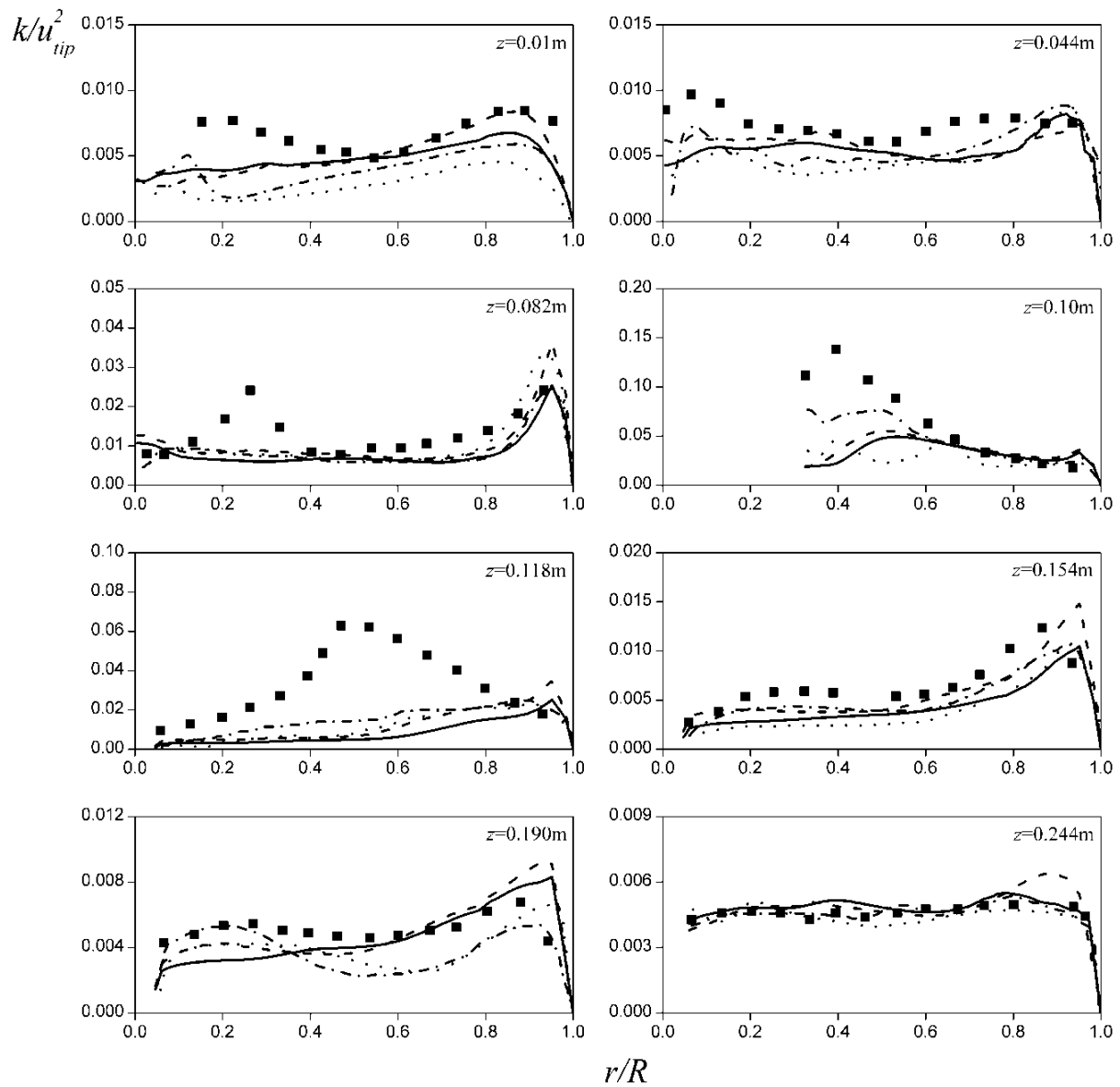
Figure 7. Comparison of the results predicted by different impeller approaches and experimental data of the dimensionless mean turbulent kinetic energy in the bulk region: experimental data (Murthy and Joshi, 2008) standard k-ε momentum source term approach predictions, RSM momentum source term approach predictions, standard k-ε SM predictions (Murthy and Joshi, 2008), RSM SM predictions (Murthy and Joshi, 2008).

Fig.7 shows the numerical comparison of turbulent kinetic energy in various positions. At z = 0.082m, it can be noticed that there are two maxima of turbulent kinetic energy, similar to the case of tangential velocity (Fig.6). They are generated by the interactions between fluid and blades a, fluid and wall, respectively. Overall, the CFD results which predicted by standard k-ε model are not satisfying, significantly underpredicting the turbulent kinetic energy at almost all positions. However, the results of momentum source term approach and SM are similar. Although RSM predictions of momentum source term approach and SM have reduced the errors, both still underestimate turbulent kinetic energy, and their results

are similar. Due to unsteady and complex nature of flow characteristics in the impeller region and the continuous conversion of kinetic energy [37], the k-ε model and RSM both fail to capture the transfer details of kinetic energy, so the momentum source term approach and SM model underpredict the turbulent kinetic energy with similar deviations when the k-ε and RSM turbulent model are applied.

From the comparisons above, it can be found that predictions of momentum source term approach with RSM turbulent model are in good agreement with the experimental data as well as SM model, although both SM and our model have some deviations in prediction of the upper part for the radial and tangential velocity. The models combined with k-ε turbulent model have less prediction accuracy, Murthy and Joshi [22] attributed these numerical errors to the overestimation of the eddy viscosity of the k-ε model. It is suggested that the standard k–ε model performs well when the flow is unidirectional that is with less swirl and weak recirculation [11, 22].

3.3. Velocity vectors

Fig.8 shows velocity vectors of the vertical plane in the middle of two baffles. It can be seen that after exerting on the momentum source, fluid velocity in the impeller region is very high, and flow gradients are large.
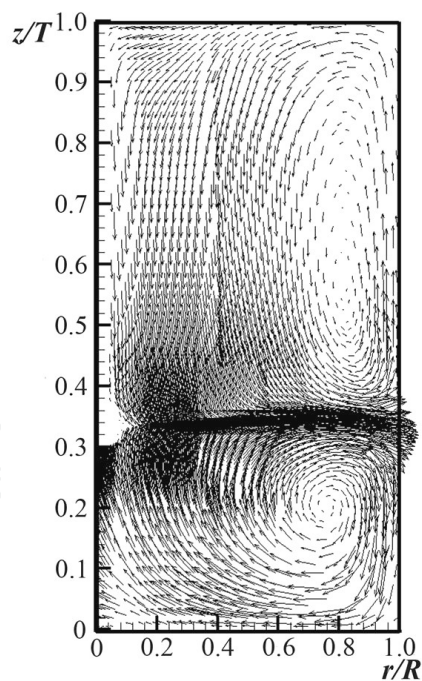

Figure 8. Velocity vectors of stirred tank in the middle plane.

As the high speed fluid jets outward, initially almost not affected by the surrounding fluid, the velocity contours are dense. The flow impinges on the tank wall, splits up into two parts and changes the direction. The split water flows at last return to impeller region and accelerated

again, repeating above-mentioned process which generates two circulation loops of different directions in the upper and lower part of the tank, respectively. It can be observed that the circulation loop ranges above the z/T value of 0.9, which is consistent with the simulations by Ng et al. [24] (1998) (Re = 40,000) and Yapici et al. [41] (2008) (Re = 60,236). Reynolds numbers of previous and present studies can ensure that the flow in a stirred vessel is fully developed turbulence, so the circulation pattern predictions can be considered properly.

Fig.9 shows the flow field of stirred tank near the impeller tip. It can be noticed that velocity distributions are not symmetrical about the impeller centre plate (z = 0.1 m), but shift upwards slightly. This result is in agreement with the previous experimental works, that the impeller is not symmetrically located, the top of the tank is a free surface, and the hub is present on the top side of the impeller [38, 42-43]. In this study, this detail has been successfully captured in the velocity field near impeller tip, further indicating that momentum source term approach prediction is in good agreement with experimental results.
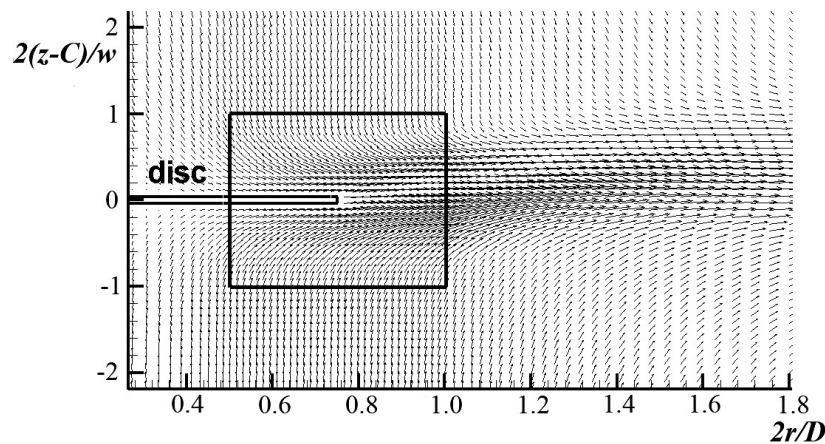

Figure 9. Velocity vectors in the middle plane near impeller tip.

3.4. Comparison of power numbers

Table 2 shows the comparison of predicted power numbers with the experimental value. Here, the experimental power numbers reported by Rushton et al. [44-45], Murthy and Joshi [22] are applied in the reference. The quantities obtained by SM model through integral ε based approach are considerably lower than the reported experimental results. Similar results have been observed in earlier studies [29, 46-47]. These deviations are usually attributed to underestimation of the turbulent quantities associated to the k–ε model [46, 48]. The power number predictions of integral power based approach in the momentum source term approach with standard k–ε model and RSM are 5.72 and 5.64, respectively, both between the experimental data 5.1 and 6.07, so they are better than those of SM.

Fig.10 shows a log-log plot of the experimentally obtained and predicted power numbers for nine kinds of Reynolds numbers which cover laminar and turbulent flow regimes. It can be observed that at lower Reynolds numbers the power numbers predicted by momentum source term approach are in good agreement with the experimental data of Rushton et al. [44].

Methods	N_P	Error/%
Experimental value (Rushton et al., 1950)	6.07	/
Experimental value (Murthy and Joshi, 2008)	5.1	/
SM torque based approach (Murthy and Joshi, 2008)	4.9	12.26
SM integral ε based approach (Murthy and Joshi, 2008)	3.9	30.17
MRF torque based approach (Deglon and Meyer, 2006)	5.40	3.31
Standard k-ε integral power based approach	5.72	2.42
RSM integral power based approach	5.64	0.98

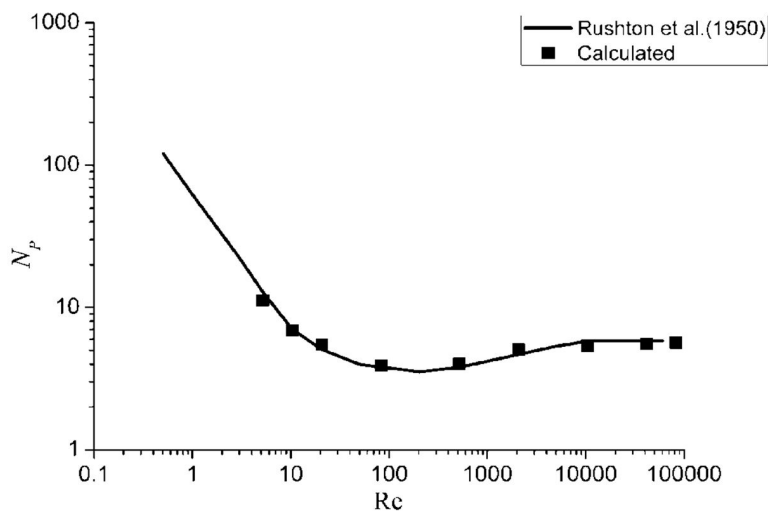**Table 2.** Power number predictions for different approaches at Re=41,467.

Figure 10. Comparison of experimental and predicted power numbers.

3.5. Computational speed

The simulations were carried out on a 100 node AMD64 cluster, each node including 2 four-core processors with 2.26 GHz clock speed and 2 GB memory. 80 processors were applied in all the computations. Present study compared the computational speeds of momentum source term approach, MRF and SM, and the required expenses are shown in Table 3. It can be seen that momentum source term approach and MRF using steady state simulations need less computational requirements than SM, and the computational time of momentum source term approach is the least.

Approach	Momentum source term	MRF	SM
Standard k-ε	48	72	340
RSM	60	86	410

Table 3. Comparison of the computational time required by different approaches, h.

4. Conclusions

An equation to predict the momentum source term is proposed without the help of experimental data in the paper. So the momentum source term approach for CFD prediction of the impeller propelling action has been developed as a tool with predictive capacity. The prediction results of the approach have been compared with the experimental data, MRF and SM model predictions in the literatures. The following conclusions can be drawn from the present work:

1. For the plate blade of the Rushton turbine stirred vessel, the tangential momentum source added by blade is proposed to be calculated by:

in which u is the linear velocity of the area element on the blade surface dS; v_θ is the fluid tangential velocity rotating with the impeller before the fluid was propelled by impeller; dS is cross-section area of the interface between fluid and the impeller blade. The radial friction force of the impeller blade is proposed to be calculated approximately (Wang et al., 2002) as following:

In which f is the friction force in the computational cells, v_r is the radial velocity of the fluid.

2. The numerical comparisons of flow field show that the momentum source term approach predictions are in good agreement with the experimental data. It has been also found that the prediction accuracy of momentum source term approach is better than MRF and similar to SM, whereas the computational time of momentum source term approach is the least of the three.

Acknowledgements

Author details

Weidong Huang[*] and Kun Li

*Address all correspondence to: huangwd@ustc.edu.cn

Department of Geochemistry and Environmental Science, University of Science and Technology of China, P. R. China

References

[1] Harvey, P. S., & Greaves, M. (1982). Turbulent-Flow in an Agitated Vessel.1. A Predictive Model. *Transactions of the Institution of Chemical Engineers*, 60(4), 195-200.

[2] Harvey, P. S., & Greaves, M. (1982). Turbulent-Flow in an Agitated Vessel.2. Numerical-Solution and Model Predictions. *Transactions of the Institution of Chemical Engineers*, 60(4), 201-210.

[3] Ranade, V. V., & Joshi, J. B. (1990). Flow generated by a disc turbine Part II: mathematical modelling and comparison with experimental data. *Institution of Chemical Engineering* [68A], 34-43.

[4] Kresta, S. M., & Wood, P. E. (1991). Prediction of the three-dimensional turbulent flow in stirred tanks. *Aiche Journal*, 37, 448-460.

[5] Luo, J. Y., Issa, R. I., & Gosman, A. D. (1994). Prediction of impeller-induced flows in mixing vessels using multiple frames of reference. Cambridge, UK. *in Proceeding of 8th Europe Conference on Mixing*, 155-162.

[6] Luo, J. Y., Gosman, A. D., Issa, R. I., et al. (1993). Full Flow-Field Computation of Mixing in Baffled Stirred Vessels. *Chemical Engineering Research & Design*, 71(A3), 342-344.

[7] Murthy, J. Y., Mathur, S. R., & Choudhary, D. (1994). CFD simulation of flows in stirred tank rectors using a sliding mesh technique. *in Proceeding of 8th Europe Conference on Mixing, Cambridge, UK*, 155-162.

[8] Mostek, M., Kukukova, A., Jahoda, M., et al. (2005). Comparison of different techniques for modelling of flow field and homogenization in stirred vessels. *Chemical Papers*, 59(6A), 380-385.

[9] Perng, C. Y., & Murthy, J. Y. (1994). A moving deforming mesh technique for simulation of flow in mixing tanks. Cambridge, UK. *in Proceeding of 8th Europe Conference on Mixing*, 37-39.

[10] Joshi, J. B., Nere, N. K., Rane, C. V., et al. (2011). Cfd Simulation of Stirred Tanks: Comparison of Turbulence Models. Part II: Axial Flow Impellers, Multiple Impellers and Multiphase Dispersions. *Canadian Journal of Chemical Engineering*, 89(4), 754-816.

[11] Joshi, J. B., Nere, N. K., Rane, C. V., et al. (2011). Cfd Simulation of Stirred Tanks: Comparison of Turbulence Models. Part I: Radial Flow Impellers. *Canadian Journal of Chemical Engineering*, 89(1), 23-82.

[12] Pericleous, K. A., & Patel, M. K. (1987). The modelling of tangential and axial agitators in chemical reactors. *Physico-chimie Chemical Hydrodynamics*, 8, 105-123.

[13] Dhainaut, M., Tetlie, P., & Bech, K. (2005). Modeling and experimental study of a stirred tank reactor. *International Journal of Chemical Reactor Engineering*, 3.

[14] Xu, Y., & Mc Grath, G. (1996). CFD predictions in stirred tank flows. *Chemical Engineering Research and Design.*, 74, 471-475.

[15] Patwardhan, A. W. (2001). Prediction of flow characteristics and energy balance for a variety of downflow impellers. *Industrial & Engineering Chemistry Research*, 40(17), 3806-3816.

[16] Revstedt, J., Fuchs, L., & Tragardh, C. (1998). Large eddy simulations of the turbulent flow in a stirred reactor. *Chemical Engineering Science*, 53(24), 4041-4053.

[17] Schneekluth, H. (1988). *Hydromechanik zum Schiffsentwurf : Vorlesungen. 3., verb. und erw. Aufl. ed., Herford: Koehler. ix*, 1076.

[18] Jiang, C. Y. (2007). *Study of several CFD models in the oxidation ditch system*, University of Science and Technology of China, Hefei, China.

[19] Jiang, C. Y., Huang, W. D., Wang, G., et al. (2010). Numerical computation of flow fields in an oxidation ditch by computational fluid dynamics model. *Environmental Science & Technology*, 33, 135-140.

[20] Gou, Q. (2008). *Numerical simulation of the propellers in oxidation ditch using Computational fluid dynamics models in Department of Earth and Space Science*, University of Science and Technology of China, Hefei.

[21] Li, B., Zhang, Q. W., Hong, H. S., & You, T. (2009). Several factors of CFD numerical simulation in stirred tank. *Chemical Industry and Engineering Progress*, 28, 7-12.

[22] Joshi, J. B., & Murthy, B. N. (2008). Assessment of standard k-epsilon, RSM and LES turbulence models in a baffled stirred vessel agitated by various impeller designs. *Chemical Engineering Science*, 63(22), 5468-5495.

[23] Deglon, D. A., & Meyer, C. J. (2006). CFD modelling of stirred tanks: Numerical considerations. *Minerals Engineering*, 19(10), 1059-1068.

[24] Ng, K., Fentiman, N. J., Lee, K. C., et al. (1998). Assessment of sliding mesh CFD predictions and LDA measurements of the flow in a tank stirred by a Rushton impeller. *Chemical Engineering Research & Design*, 76(A6), 737-747.

[25] Ding, Z. R. (2002). *Hydrodynamics*, Beijing, China, Higher Education Press.

[26] Schneekluth, H. (1997). *Hydromechanik zum schiffsentwurf*, Herford, Koehler Book Company, 3, In Chinese, translated by Xian P.L., Shanghai, China: Publishing company of Shanghai Jiao Tong University, 1988.

[27] Wang, Y. D., Luo, G. S., & Liu, Q. (2002). *Principles of transport processes in chemical engineering*, Beijing, China, Tsinghua University Press.

[28] Wechsler, K., Breuer, M., & Durst, F. (1999). Steady and unsteady computations of turbulent flows induced by a 4/45 degrees pitched-blade impeller. *Journal of Fluids Engineering*, 121, 318-329.

[29] Montante, G, Coroneo, M, Paglianti, A, et al. (2011). CFD prediction of fluid flow and mixing in stirred tanks: Numerical issues about the RANS simulations. *Computers & Chemical Engineering*, 35(10), 1959-1968.

[30] Aubin, J., Fletcher, D. F., & Xuereb, C. (2004). Modeling turbulent flow in stirred tanks with CFD: the influence of the modeling approach, turbulence model and numerical scheme. *Experimental Thermal and Fluid Science*, 28(5), 431-445.

[31] Launder, B. E., & Spalding, D. B. (1974). Numerical computation of turbulent flows. *Computer Methods in Applied Mechanics and Engineering*, 3, 269-289.

[32] Speziale, C. G., Sarkar, S., & Gatski, T. B. (1991). Modelling the pressure-strain correlation of turbulence: an invariant dynamical systems approach. *Journal of Fluid Mechanics*, 227, 245-272.

[33] Brucato, A. M. C. F. G., et al. (1998). Numerical prediction of flows in baffled stirred vessels: a comparison of alternative modelling approaches. *Chemical Engineering Science*, 53, 3653-3684.

[34] Bartels, C., Breuer, M., Wechsler, K., et al. (2002). Computational fluid dynamics applications on parallel-vector computers: computations of stirred vessel flows. *Computers & Fluids*, 31(1), 69-97.

[35] Xuereb, C., & Bertrand, J. (1996). D hydrodynamics in a tank stirred by a double-propeller system and filled with a liquid having evolving rheological properties. *Chemical Engineering Science*, 51(10), 1725-1734.

[36] Shekhar, S. M., & Jayanti, S. (2002). CFD study of power and mixing time for paddle mixing in unbaffled vessels. *Chemical Engineering Research & Design*, 80(A5), 482-498.

[37] Line, A., & Escudie, R. (2003). Experimental analysis of hydrodynamics in a radially agitated tank. *Aiche Journal*, 49(3), 585-603.

[38] Wu, H, & Patterson, G.K. (1989). Laser-doppler measurements of turbulent flow parameters in a stirred mixer. *Chemical Engineering Science*, 44, 2207-2221.

[39] Murthy, B. N., & Joshi, J. B. (2008). Assessment of standard k-ε, RSM and LES turbulence models in a baffled stirred vessel agitated by various impeller designs. *Chemical Engineering Science*, 63, 5468-5495.

[40] Yianneskis, M., Popiolek, Z., & Whitelaw, J. H. (1987). An experimental study of the steady and unsteady flow characteristics of stirred reactors. *Journal of Fluid mechanics*, 175, 537-555.

[41] Yapici, K., Karasozen, B., Schafer, M., et al. (2008). Numerical investigation of the effect of the Rushton type turbine design factors on agitated tank flow characteristics. *Chemical Engineering and Processing*, 47, 1340-1349.

[42] Stoots, C. M., & Calabresc, R. V. (1995). Mean velocity field relative to a rushton turbine blade. *Aiche Journal*, 41, 1-11.

[43] Derksen, J. J., Doelman, M. S., & Van den Akker, H. E. A. (1999). Three-dimensional LDA measurements in the impeller region of a turbulently stirred tank. *Experiments in Fluids*, 27(6), 522-532.

[44] Rushton, J. H., Costich, E. W., & Everett, H. J. (1950). Power Characteristics of Mixing Impellers.1. *Chemical Engineering Progress*, 46(8), 395-404.

[45] Rushton, J. H., Costich, E. W., & Everett, H. J. (1950). Power Characteristics of Mixing Impellers.2. *Chemical Engineering Progress*, 46(9), 467-476.

[46] Kukukova, A., Mostek, M., Jahoda, M., et al. (2005). CFD prediction of flow and homogenization in a stirred vessel: Part I vessel with one and two impellers. *Chemical Engineering & Technology*, 28(10), 1125-1133.

[47] Uludag, Y., Yapici, K., Karasozen, B., et al. (2008). Numerical investigation of the effect of the Rushton type turbine design factors on agitated tank flow characteristics. *Chemical Engineering and Processing*, 47(8), 1346-1355.

[48] Sommerfeld, M., & Decker, S. (2004). State of the art and future trends in CFD simulation of stirred vessel hydrodynamics. *Chemical Engineering & Technology*, 27(3), 215-224.